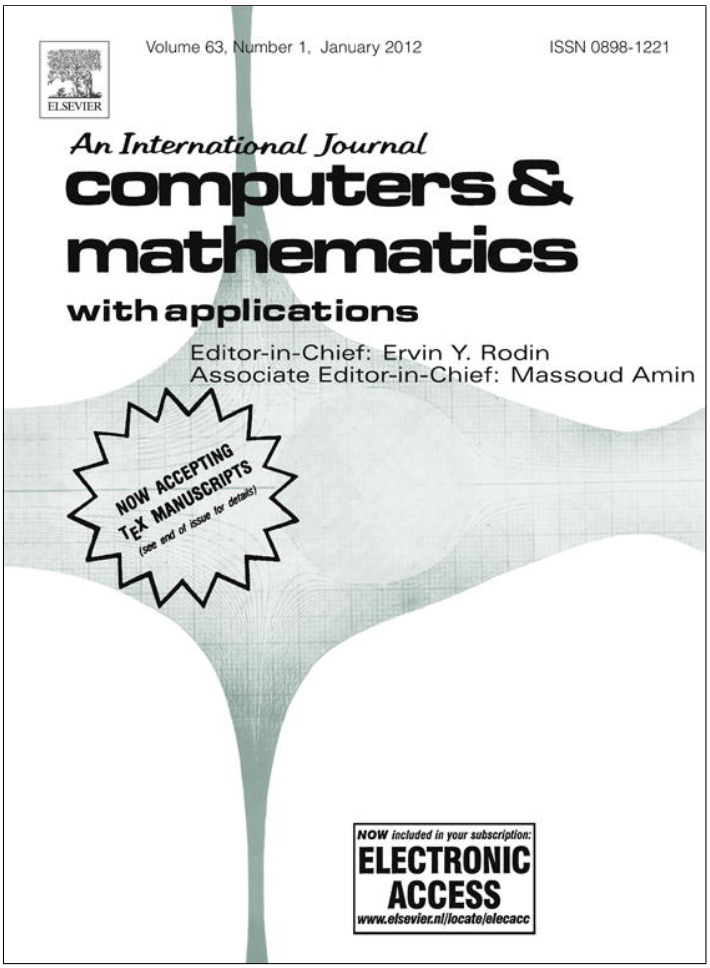

Computers and Mathematics with Applications 63 (2012) 68–82

Contents lists available at SciVerse ScienceDirect

Computers and Mathematics with Applications

journal homepage: www.elsevier.com/locate/camwa

Fuzzy wavelet network identification of optimum operating point of non-crystalline silicon solar cells

Syafaruddin [a,*], Engin Karatepe [b], Takashi Hiyama [c]

[a] Department of Electrical Engineering of Universitas Hasanuddin, 90245 Tamalanrea-Makassar, Indonesia

[b] Department of Electrical and Electronics Engineering of Ege University, 35100 Bornova-Izmir, Turkey

[c] Department of Computer Science and Electrical Engineering of Kumamoto University, 2-39-1 Kurokami, Kumamoto 860-8555, Japan

ARTICLE INFO

Article history:
Received 5 October 2010
Received in revised form 28 October 2011
Accepted 28 October 2011

Keywords:
Fuzzy-wavelet network
Solar cell
Photovoltaic
System identification
Maximum power point

ABSTRACT

The emerging non-crystalline silicon (c-Si) solar cell technologies are starting to make significant inroads into solar cell markets. Most of the researchers have focused on c-Si solar cell in maximum power points tracking applications of photovoltaic (PV) systems. However, the characteristics of non-c-Si solar cell technologies at maximum power point (MPP) have different trends in current–voltage characteristics. For this reason, determining the optimum operating point is very important for different solar cell technologies to increase the efficiency of PV systems. In this paper, it has been shown that the use of fuzzy system coupled with a discrete wavelet network in Takagi–Sugeno type model structure is capable of identifying the MPP voltage of different non-c-Si solar cells with very high accuracy. The performance of the fuzzy-wavelet network (FWN) method has been compared with other ANN structures, such as radial basis function (RBF), adaptive neuro-fuzzy inference system (ANFIS) and three layered feed-forward neural network (TFFN). The simulation results show that the single FWN architecture has superior approximation accuracy over the other methods and a very good generalization capability for different operating conditions and different technologies.

1. Introduction

Intelligent systems by means of the artificial neural network and fuzzy logic methods have been satisfactorily used to solve the tasks of modeling, identification, optimization, prediction, forecasting and control of complex systems in different fields of application. In general, determining the architecture of a neural network or constructing the fuzzy rules are uncertain and take more time to find the best structure to improve the generalization capability in system identification problems [1–3]. Intelligent methods are generally applicable to solve the engineering problems due to their symbolic reasoning, flexibility and the explanation capabilities. Moreover, they are capable of handling and learning the non-linear, large, complex and even incomplete data patterns. On the other hand, wavelets with neural network and fuzzy systems have been used in system identifications [3–10]. A wavelet offers multiresolution decomposition to separate components of a function for improving the analysis. Once the training of these is performed, they can give the estimation and generalization at high accuracy. In comparison with the standard linear model for optimization methods, the ANN methods provide a compact solution for multi-variable problems and they do not require the knowledge of internal system parameters [5]. Since only a training process is required and the output parameters are directly determined without solving any non-linear mathematical equations or statistical assumptions as in the conventional optimization methods, these tools have been used

* Corresponding author. Tel.: +62 411 588111; fax: +62 411 590125.
E-mail address: syafaruddin@unhas.ac.id (Syafaruddin).

0898-1221/$ – see front matter © 2011 Elsevier Ltd. All rights reserved.
doi:10.1016/j.camwa.2011.10.073

in many engineering applications [1]. For these reasons, the ANN methods are suitably proven for solving the optimum points of PV systems where their output power characteristics are non-linear and intermittent [11,12]. It is well-known that the PV system characteristic is non-linear due to the natural behaviors of semiconductor materials inside the solar cell and this characteristic cannot be simply expressed by a single equation in order to deal with all operating conditions or different solar cell technologies. Also, the trajectory of optimum points of the PV system is changing dramatically due to some factors, such as irradiance level, ambient temperature, mismatching cell, array configuration and partial shading.

As the mature optimization techniques, different ANN architectures have been proposed to solve a variety of problems in the PV system application so far [13–27]. They are radial basis function (RBF) neural network, adaptive neuro-fuzzy inference system (ANFIS), three layered feed-forward neural network (TFFN) and wavelet network methods. These structures may have their own advantages as well as disadvantages over the others in different applications. In [13], the use of adaptive wavelet-network architecture in finding a suitable forecasting model for predicting the daily total solar-radiation is investigated. RBF neural network structure is used to determine the voltage reference for the MPPT controller [14]. It was also reported in [15], that the RBF method has structural simplicity and universal approximation to estimate the solar irradiation. The RBF method is able to reduce the computational effort by combining with the genetic algorithm (GA) to minimize the total capacity and total capital cost of the energy storage system [16,17]. Also, the RBF method combined with a neuro-fuzzy regulator has been used to increase the efficiency of the PV system [18]. The RBF neural network is identified as a very strong network with fast training process and the structure is directly confirmed after training. However, there might be trivial errors in the RBF method during the validation process, such as the over fitting condition. On the other hand, the ANFIS model has been used to train individually on each component of the PV power system under variable climate conditions [19]. The ANFIS network has the high adaptive control performance and robustness for the tracking system and MPPT control for the efficient improvement of the photovoltaic system [20]. The ANFIS method is also a very strong network with high accuracy output during the training and testing process. The accuracy of this method is likely to depend on the type and number of membership functions for the input signals. However, this network is generally designed for a single output. Therefore, for multi-objective optimization problems, it requires a multi ANFIS network and each network must be separately trained. For the TFFN method, this structure is the most popular method in solving different problems in PV application. This method has been used to optimize the duty ratio of buck-boost converter taking the environmental factors as the input signals [21–23]. The TFFN method is also combined with other techniques like the GA to determine the optimal power dispatch under random load [24], with a heuristic approach to optimize operating costs of a representative PV based microgrid system [25] and with evolutionary programming to quantify the optimum values of a number of hidden nodes for the prediction of energy output of a grid connection PV system [26]. The TFFN network has a simple structure, however it may end up with a certain computational burden that needs the intuitive decision of users to determine the best network structure. The common problem of this method is too many possible network structures that can be selected during the training process [27].

On the other hand, the combination of wavelet theory and fuzzy system has led to the development of a simple algorithm based on the wavelet functions at the then parts of the fuzzy logic rules. The constructed fuzzy rules can be adjusted by learning the discrete wavelet transform parameters of the selected wavelets and also determining the shape of membership functions. The applications of fuzzy-wavelet networks in the PV system application are very rare. Only Ref. [13] has utilized a wavelet based neural network model for forecasting daily total solar radiation and the results show that this method has high classification and identification abilities, simple structure, less training time, adjustable performance and requires a smaller number of iterations when compared with other neural networks.

This paper presents the eminence of fuzzy wavelet network model over the other ANN structures to identify the optimum operating points of non-crystalline Silicon solar cells. This study is inspired from the previous work presented in [3], especially for the second proposed FWN where the fuzzy model uses the discrete wavelet transform completely except the scaling function. From numerical experiments in this previous study, it is identified that the FWN method has high function approximation accuracy, fast convergence and quick learning ability. The reason of selecting the target study of non-c-Si solar cells is the fact that the researchers are still concentrating on modeling and simulating the c-Si based technology [28], while solar cell technology is rapidly developing where the non c-Si solar cells are entering the PV market. The only modeling of spectral effects on the short-circuit current of a-Si solar cell as one of the non c-Si technologies can be found in [29]. Moreover, the characteristic of optimum operating points, especially the optimum voltage of non-c-Si is totally different from conventional silicon solar cell technologies. For example, under constant temperature, the optimum voltage may increase until a certain irradiation level, and then will start decreasing after that. The nonlinear relationships are given in the following sections. From these viewpoints, this study is focused on following the optimum operating voltage. In a voltage based maximum power point tracking (MPPT) controller [23,30,31], the determination of optimum voltage as a reference signal is very important. Once the optimum voltage can be identified, it ensures that the PV system can be operated optimally at the rated conversion efficiency.

This paper is organized into several sections. Section 2 provides the characteristic of voltage at maximum power points in different non c-Si PV modules technologies. Then, Section 3 explains the fuzzy wavelet network structure and compares the performance of the FWN with other wavelet neural networks (WNN) and FWN for a single variable benchmark function. Section 4 presents the comparison performance with different conventional ANN structures include some simulation results for estimating an optimum operating point of different PV module technologies under various scenarios. Finally, the conclusion will be drawn in Section 5.

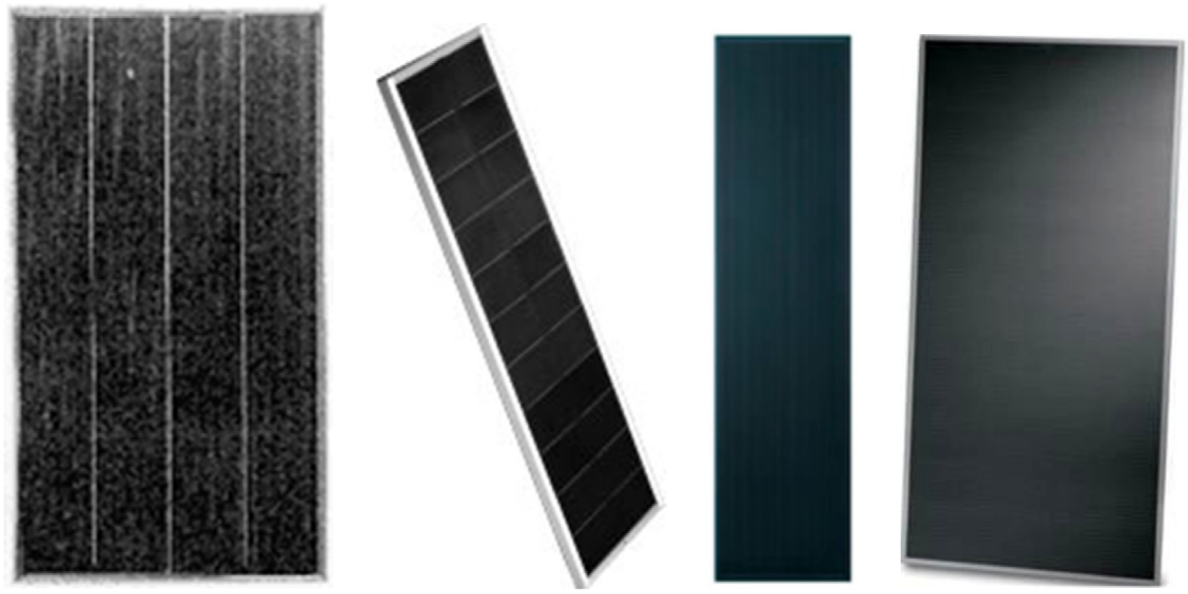

(a) Solarex MST-43MV. (b) USSC UniSolar US-32. (c) Siemens ST-40. (d) First Solar FS-50.

Fig. 1. The physical appearance of PV modules.

Table 1
Specification of PV modules under 1000 W/m^2 and 25 °C.

PV modules	$I_{SC}[A]$	$V_{OC}[V]$	$I_{MPP}[A]$	$V_{MPP}[V]$	$P_{MPP}[W]$
MST-43	0.787	101.0	0.616	71	43.74
US-32	2.4	23.8	1.94	16.5	32.01
ST-40	2.59	22.2	2.41	16.6	40.00
FS-50	1.0	90	0.77	65	50.05

2. Characteristic of voltage at maximum power points in different non c-Si PV modules technology

Development of solar cell technology has been rapidly increasing since the last decade [32]. Crystalline Si solar cells are the current mainstream in the market, but sales have been significantly expanded for non c-Si solar cells due to the development of nano-material technology. The main reason of this trend is to cut the manufacturing cost of conventional Si technology. The non-Si solar cells can be found much more cheaply than Si based solar cells for the same efficiency conversion, especially under massive production of cells. Other profiles are that the non c-Si solar cell technologies have low cost, are lightweight, flexible and more versatile with a very small amount of silicon needed. The energy payback of this technology is very fast, possibly within 2 months, compared with 4 years for conventional Si technology. In the end, the non c-Si solar cell technologies have the potential to be inexpensive to produce and they could dominate future global production.

In this study, four different types of PV module; Solarex MST-43MV (2*j* a-Si), USSC UniSolar US-32 (3*j* a-Si), Siemens ST-40 (CIS) and First Solar FS-50 (thin film CdTe) are used. The specification of PV modules under 1000 W/m^2 and 25 °C is presented in Table 1. The Solarex MST-43MV and USSC UniSolar US-32 PV modules are the tandem junction and triple junction thin-film module amorphous silicon cells, respectively. These modules were designed for the purpose of effectively using the conversion of sunlight spectrum. The bottom cell absorbs red light, the middle cell absorbs green light and the top cell absorbs the blue light. In the tandem junction technology, solar cells are developed by depositing semiconductor alloys in thin layers on glass. The major development in this cell is in their efficiency and stability. The tandem-junction structure stacks two or three solar cells vertically, with each cell tuned for optimum conversion of different segments of the spectrum. On the other hand, Siemens ST-40 and First Solar FS-50 are CIS and thin film CdTe PV modules, respectively. The ST-40 module is composed of a monolithic structure of series-connected Copper Indium Diselenide (CIS) based solar cells. These multiple-layer cells are characterized by exceptional spectral response and long-term performance integrity. The ST-40 performance efficiency is almost similar to crystalline photovoltaic modules. The last module with CdTe based thin-films technology is recommended when high output voltage is desired. This module uses very thin layers of compound semiconductor material with low temperature coefficients which provides for cost effective and greater energy production. The physical appearance of these PV modules is given in Fig. 1.

These PV modules are modeled following the I–V curve characteristic model developed by Sandia National Laboratory [33,34]. This model is suitable to represent the electrical performance on different commercial PV modules. The important characteristic is explained as follows. The short-circuit current depends linearly on the solar irradiation; on the other

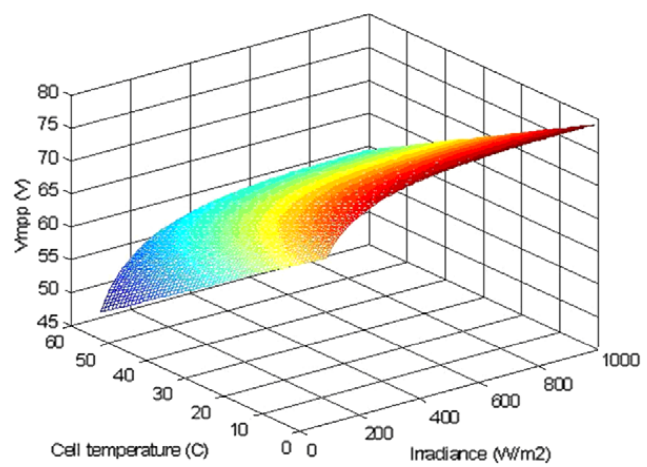

(a) Solarex MST-43MV (2*j* a-Si).

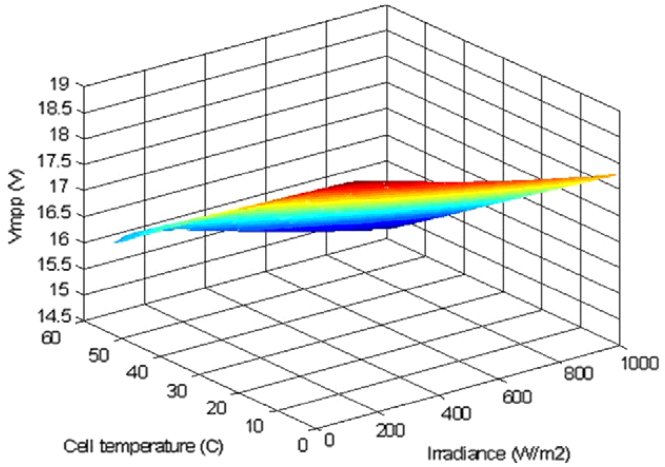

(b) USSC UniSolar US-32 (3*j* a-Si).

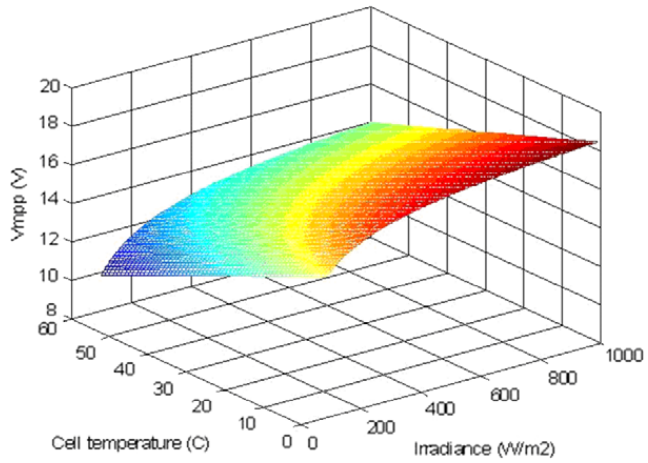

(c) Siemens ST-40 (CIS).

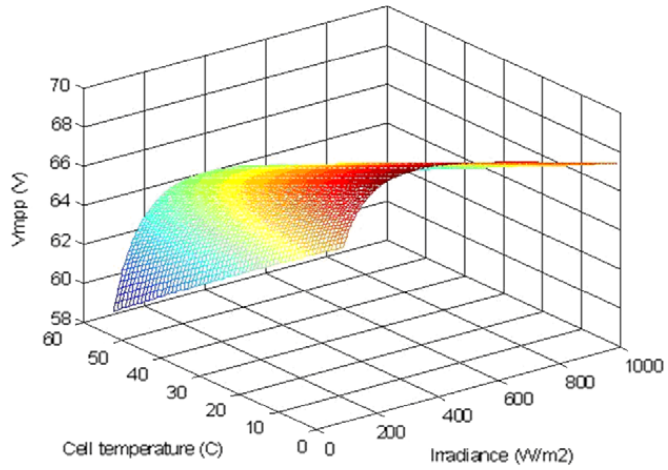

(d) First Solar FS-50 (thin film CdTe).

Fig. 2. Voltage at maximum power point (V_{MPP}) for irradiance (100–1000 W/m^2) and cell temperature (10–60 °C).

hand, the open-circuit voltage depends logarithmically on the solar irradiation. These two parameters are also dependant on cell temperature. As temperature increases, the open circuit voltage decreases following the p–n junction voltage temperature dependency as seen in the diode factor. Due to this reason, the solar cells have a negative temperature coefficient of open-circuit voltage. The short-circuit current is proportional to temperature. When temperature increases, the current also increases because more photons are absorbed by the semiconductor material. However, under this condition, the decrease in voltage is much higher than the increase in current. Therefore, the output power will be decreased as temperature is increased. These kinds of relationships are almost similar in short-circuit current and open-circuit voltage for all semiconductor types of solar cells. However, there might be different characteristics at maximum power point voltage (V_{MPP}). The V_{MPP} characteristics are shown in Fig. 2. It can be seen from this figure that the correlation between the optimum voltage and irradiance/cell temperature for each module is non-linear. In this respect, to operate the PV modules at their maximum power point, tracking the optimum voltage using an intelligent technique by means of a functional reasoning method for function approximation is totally necessary. In the following sections, this will be clearly explained.

3. Fuzzy wavelet network structure and algorithm

Nonlinear system identification has been of interest in scientific research and engineering applications. Artificial neural networks and fuzzy logic systems are widely used as an effective approach for modeling and solving non-linear systems. Both methods offer a potential that is conceptually easy to understand and more flexible to model nonlinear functions of arbitrary complexity. The one hidden layer feedforward network with trained backpropagation family algorithms is gaining broad acceptance due to its simplicity and expressiveness power. The backpropagation algorithm can fall into a local minimum and converge slowly in some applications. Wavelet-based analysis is an exciting new problem solving tool for the mathematician, scientist, and engineer [35]. Discrete wavelet transform can decompose a signal at different independent scales and does it in a very flexible way. Because of that it can be used as the basis for robust numerical algorithms [36]. In this section,

the structure of the FWN that consists of a set of fuzzy rules is described [3]. The FWN might avoid a local minimum. For practical implementations, infinite wavelet frames must be truncated into finite sets.

The fuzzy rule has a form as follows;

$$R_j\text{: IF } x_1 \text{ is } A_{j,1} \text{ AND } x_2 \text{ is } A_{j,2} \text{ AND } \ldots x_n \text{ is } A_{j,n} \text{ THEN } y_j = \sum_{k=-L}^{L} f_k(x) \quad j\text{: } 1, 2, \ldots, M \tag{1}$$

where

$$f_k(x) = \sum_{m=0}^{K} d_{j,k,m} \prod_{i=1}^{n} 2^{m/2} \psi(2^m x_i - k). \tag{2}$$

The variables m and k are integers that scale and translate the mother function, $\psi(x)$, to generate a family of discrete wavelets. The scale index m indicates the wavelet's width, and location index k gives its position. For each increasing index m, a higher or finer resolution function is added, which adds increasing detail [35,36]. The FWN has a different structure and each rule consists of $(K + 1) * (2 * L + 1)$ wavelet functions. For this structure, where M, L, and K are fixed parameters and expansion coefficients $(d_{j,k,m})$ are free parameters to be tuned when mapping the input–output relationship. The parameters L and K determine the size of the wavelet for the jth fuzzy rule. For this FWN, the Mexican Hat wavelet function $\psi(x) = (1 - 2x^2)\exp(-x^2)$ was selected as our wavelet function.

In the second stage of the FWN, the inputs of a system are codified into linguistic values, the set of Gaussian membership functions attributed to each variable. The third stage calculates to each rule R_j its respective activation degree. The FWN systems have a mathematical model that resembles that of a three-layer network, fuzzification, fuzzy inference, and defuzzification [3]. By applying fuzzy product inference engine, singleton fuzzifier, center average defuzzifier, and the Gaussian membership functions process, the output of FWN becomes:

$$y = \frac{\sum_{j=1}^{M} \prod_{i=1}^{n} \mu_{j,i}(x_i) y_{j,i}(x_i)}{\sum_{j=1}^{M} \prod_{i=1}^{n} \mu_{j,i}(x_i)} \tag{3}$$

where $\mu_{j,i}(x) = \exp(-((x - xc_{j,i})/\sigma_{j,i})^2)$, $xc_{j,i}$ denote the centers and $\sigma_{j,i}$ denote the standard deviation for the membership function associated with rule j. After determination of the structure, the next step is to optimize the network's parameters. In this network, the centers of fuzzy membership function, standard deviations of membership function and expansion coefficients of wavelet function are free parameters, consequently the total free unknown parameter number is $2 * n * M + M * ((2 * L + 1) * (K + 1))$, where M and n are fuzzy rule number and variable number of the function respectively. The designing fuzzy system is now equivalent to determining these parameters. In this work, our task is to design the fuzzy wavelet system $y(x)$ in the form of Eq. (3) such that the matching error

$$E = \frac{1}{2} \sum_{p=1}^{N} (y(x^p) - y_d^p)^2 \tag{4}$$

is minimized, where N is the length of input–output pairs and y_d^p is desired output value at x^p. That is, the task is to determine the free parameters such that E of (4) is minimized. To determine these parameters, the fuzzy system is represented as a feedforward network. Levenberg–Marquardt (LM) algorithm Fletcher strategy is used for tuning these parameters. The entire value of a given system is normalized between -1 and $+1$. The system parameters were initialized to linearly equally spaced points between 0 and 1. Only the membership function's standard deviation parameters were initialized to 1. The learning algorithm of the used FWN can be summarized in Fig. 3.

Since the given system is normalized, a dimensionless performance index (J) formulated as follows is introduced for performance measurement during the testing,

$$J = \sqrt{\frac{\sum_{i-1}^{N} (y_i - y_i^d)^2}{\sum_{i}^{N} (y_i^d - \bar{y})^2}} \quad \text{with } \bar{y} = \frac{1}{N} \sum_{i=1}^{N} y_i^d \tag{5}$$

where N is the number of the parameter data set, i is the ith sample of data, y_i^d is the desired output and y_i is the estimated output from FWN.

In the literature, several fuzzy and neural wavelet networks have been proposed for several functions [36–48]. In this paper, the performance of the FWN with other WNN and FWN can be seen in Table 2 for the below single variable benchmark

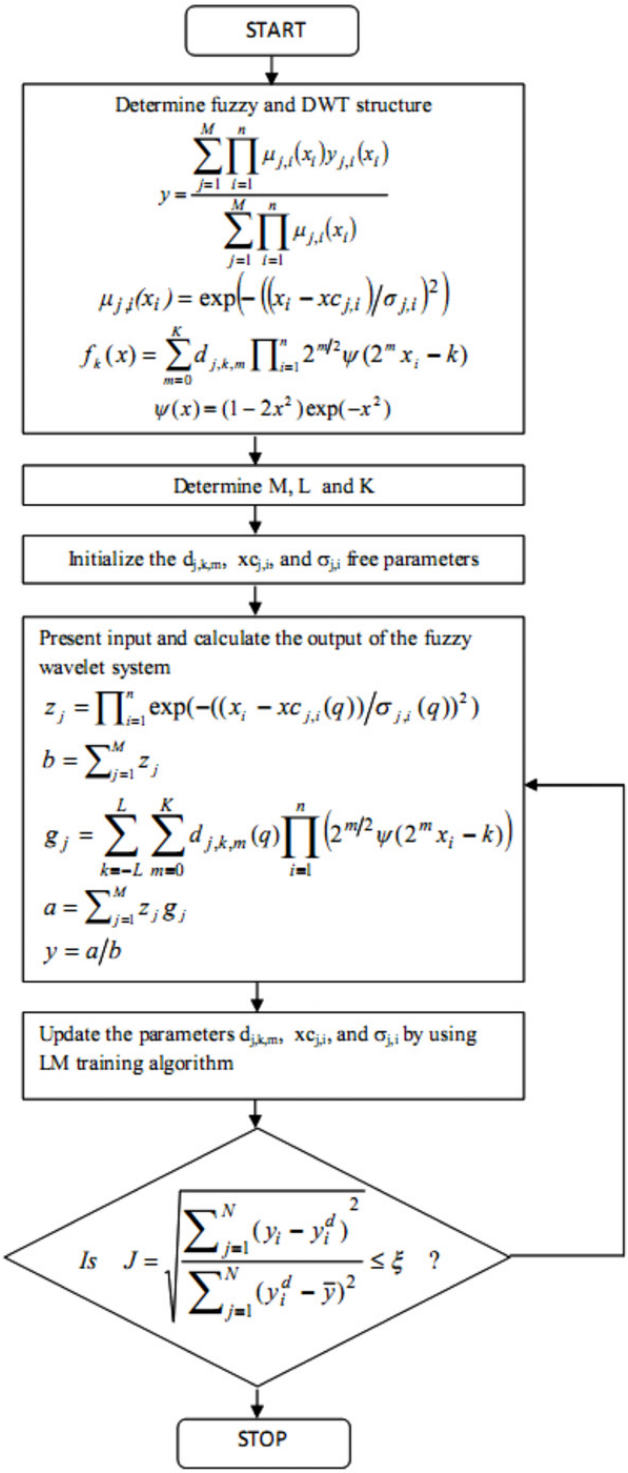

Fig. 3. The algorithm of constructing the FWN.

function (6), which is one of the important examples on wavelet networks. A data set of 200 input–output pairs is used for training and testing of the FWN. Both training data and testing data are normalized in the interval $[-1, 1]$.

$$f(x) = \begin{cases} -2.186x - 12.864 & -10 \le x < -2 \\ 4.246x & -2 \le x < 0 \\ 10\exp(-0.5x - 0.5)\sin(x(0.03x + 0.7)) & 0 \le x < 10. \end{cases} \tag{6}$$

Since the piecewise functions have been used widely, performance comparison with obtained accuracy by other researches was made by using the non-dimensional error index (5).

Table 2
Comparison of different models for the benchmark function.

Model	Performance index (J)	References
Zhang and Beveniste	0.05057	[4]
Chen and Bruns	0.0480	[36]
Yao et al.	0.03	[37]
Song and Qi	0.04	[38]
Safavi et al.	0.0072	[39]
Ho et al.	0.021	[40]
Srivastava et al.	0.0108	[41]
Srivastava et al.	0.0014	[41]
Karatepe and Alci	0.00957	[3]
Wang et al.	0.03	[42]
Sadati and Marami	0.00101	[43]
Singh et al.	0.0093	[44]
Singh et al.	0.0006	[44]
Tzeng	0.0303	[45]
Ebadat et al.	0.0071	[46]
Zainuddin and Pauline	1.90974e − 014	[47]

4. Performance comparison for optimum operating point of PV modules

In this section, the performance of FWN is compared with three different ANN structures, for instance radial basis function (RBF) neural network, adaptive neuro-fuzzy inference system (ANFIS) and three layered feed-forward neural network (TFFN) for estimating optimum operating points of different PV module technologies. The configurations have two input signals; irradiance level (E) and cell temperature (T_c) and a single output signal; MPP voltage (V_{MPP}). The network configurations and epoch number are determined according to the performance index (J). For that case, the desired output is the ideal voltage at maximum power point (V_{MPP}), V_{op} is the estimated optimum voltage and $\overline{V}_{MPP}$ is the average of V_{MPP}. There are 228 numbers of training data sets, between 100–1000 W/m^2 and 10–65 °C, to cover the entire domain problems as $V_{MPP} = f(E, T_c)$. The trainings were terminated when the error of the test sets were beginning to increase.

In theoretical manner, there can be an unlimited number of unknown parameters in an intelligence system. However, when mapping an input–output data by using an ANN based method, the number of the parameters should be kept reasonably small for successful identification of a structure, avoiding exponential computational complexity. In other words, this means that the computational effort depends upon the number of unknown parameters, but nevertheless a greater number of free parameters does not mean that a desired approximation accuracy of a network can be obtained. For this reason, we will observe and discuss the performance of the ANN methods by increasing the number of parameters to get enough estimation accuracy.

The RBF neural network is a typical neural network structure using local mapping instead of global mapping as in multi layer perceptron (MLP) [49]. In the MLP method, all inputs cause an output, while in the RBF method; only inputs near a receptive field produce an activation function. The hidden layer is locally tuned neurons centered over receptive fields. Receptive fields are located in the input space areas where input vectors exist. If an input vector lies near the center of a receptive field, then that hidden layer will be activated. The training process using an RBF network is very simple. Once the goal error is set, the training is stopped and the number of hidden nodes is confirmed. The epoch for training in an RBF network depends on the complexity of input–output relationships. If they are simple, then the training is terminated with a small number of neurons, or vice versa. In this study, the training iteration number (epoch) is set between 25 and 30 and depends on the type of PV modules. In the training process, the hidden nodes are obtained by adding one by one neuron in time until the performance of the network falls beneath an error goal. In this study, the parameter of the training process: the mean squared error goal (GOAL), spread of radial basis functions (SPREAD), maximum number of neurons (MN) and the number of neurons to add between displays (DF) are 0.003, 1.0, 228, 1, respectively.

Fig. 4 shows the typical results of the performance index to the number of parameters for the RBF network during the training process of different PV module types. This figure confirms that the training process using an RBF network for Solarex MST-43MV (2*ja*-Si) is showing the smallest error (0.018943) compared with other PV module types. In fact, to reach this good result requires 2 times more hidden nodes than other PV modules. The performance index of this module after 200 numbers of parameters is 0.018943, compared with 0.086174, 0.120026 and 0.165788 for FS-50, ST-40 and US-32 PV modules, respectively. A very unstable performance of the RBF structure occurs in US-32.

The ANFIS network is especially designed for single output, called Sugeno type fuzzy inference systems (FIS). This method is considered as a hybrid learning algorithm because it combines the least-squares and backpropagation gradient descent methods for training parameters of FIS membership functions. The training process using the ANFIS method is very fast and the network structure is also directly confirmed. During the training process, once the number of epochs is reached, then the training is stopped. In this study, the best number of epochs is 20. The small number of epochs leads to the fast training process using the ANFIS network. That is way the ANFIS method is claimed to be faster compared with other methods. The important structure of the ANFIS network is the type and number of membership functions for each input signal. In this

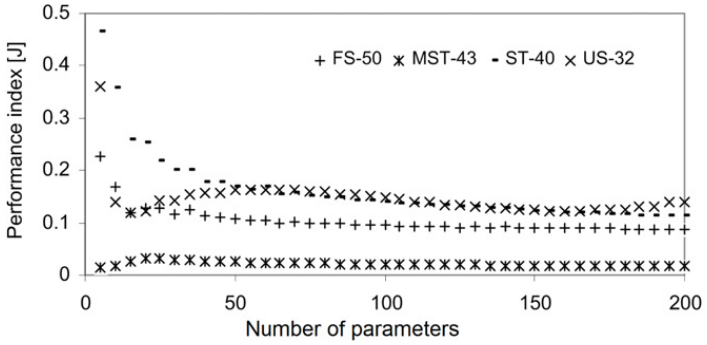

Fig. 4. Training performance index versus number of parameters for the RBF network.

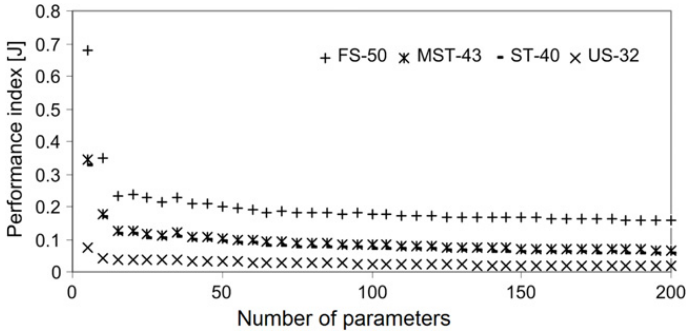

Fig. 5. Training performance index versus number of parameters for the ANFIS network.

study, the generalized bell membership function 'gbellmf' is set for each input. More accuracy can be reached using this network by adding the number of membership functions for each input, but the simulation progress becomes very slow.

Fig. 5 presents the performance index result during the training process using the ANFIS network for different PV module types. It is clear from this figure that this ANN structure is more suitable for US-32 where the lowest error of 0.015515 compared with other PV module types. This result implies that this method can overcome the problem during the training process as in RBF network. The similar performance can be found for MST-43MV and ST-40 using the ANFIS network. However, the highest training error still occurs in FS-50 PV modules when using the ANFIS network.

The remaining ANN structure is the TFFN method. This method uses backpropagation gradient descent methods for adjusting the weights in order to reduce the learning error [50]. Once the error gradient is calculated, the weights are adjusted. In this method, there are many possibilities to construct this network. Therefore, the selection of network structure is based on the intuitive thinking of the trainer. In this respect, the training process takes much time. In this study, when the 'logsig' function utilized an activation function between layers, the performance became better than the other types of activation functions. Other important factors during the training of the TFFN network are the learning and momentum rates. The learning rate means how much the weight is changed at each step. If this rate is too small, the output training will be very precise, but the algorithm will take a long time to converge. On the other hand, if too large, the outputs will be bouncing around and the algorithm may diverge. The momentum rate is related to the time when the weights are updated. This rate is commonly determined by trial and error [51]. In this study, the learning and momentum rate are specified to 0.2 and 0.85, respectively. In addition, the training process using the TFFN network could be very slow due to the very high number of epochs to be set. To reach such outcomes in this study, the epoch number is specified at 50,000.

Fig. 6 depicts the performance of the TFFN network during the training process for all PV modules. This ANN network seems not suitable with FS-50 module because of instability during the training process and the highest error training of 0.100284, compared with other PV modules. In addition, it requires high number of hidden nodes for this performance outcome. Almost the same training performance is obtained for remained PV modules using this TFFN network.

For these results, it is very difficult to consider that a single ANN structure is robust to all PV module types. One structure may good for one type of module but not for other ones, since the networks can be trapped in a local minimum according to initial parameter values and configurations. It is very difficult to find the best initial values for each network to avoid the local minimums. On the other hand, as can be seen in Figs. 4–6, it is difficult to say that if the number of parameters is increased the best structure can be obtained for each case. In addition, searching the best configuration for each system it takes a very long time during the training process of networks. These kinds of problems can be overcome by using a FWN structure as a novel approximate tool. The performance of the used FWN network during the training process can be seen in Fig. 7. As can be seen in the figure, when the number of unknown parameters increases, the performance of the FWN

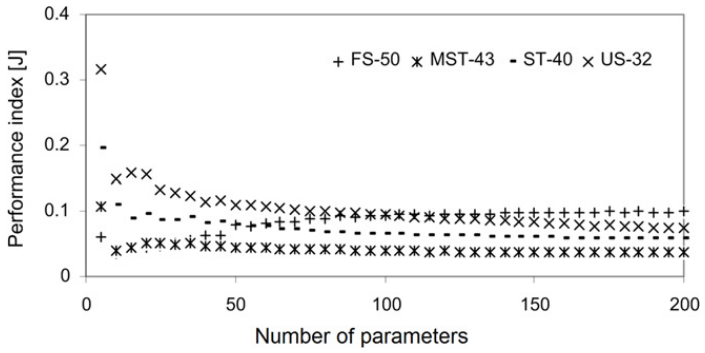

Fig. 6. Training performance index versus number of parameters for the TFFN network.

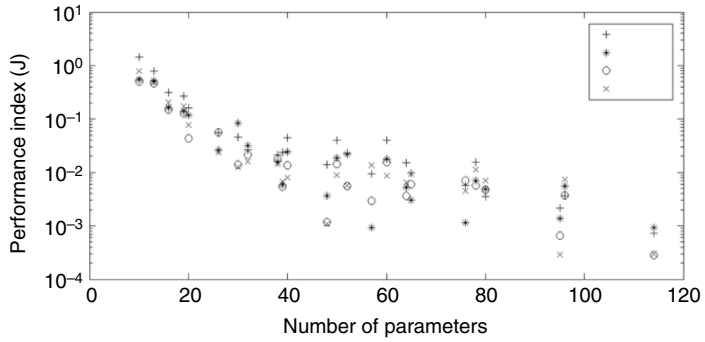

Fig. 7. Training performance index versus number of parameters for the FWN network.

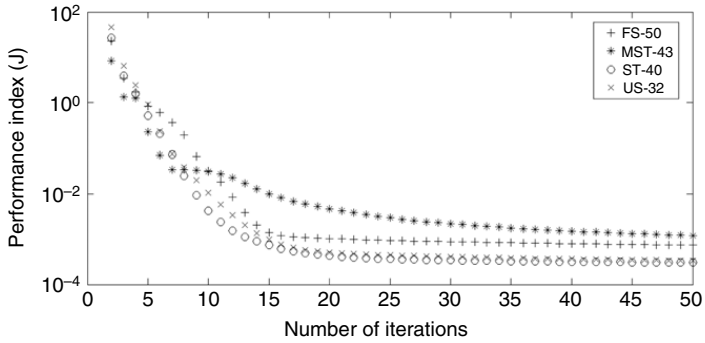

Fig. 8. Training performance index versus number of iterations for the FWN network.

is getting better. Wavelets represent a special class of functions that can generate bases in functional vector spaces. If the numbers of wavelets or fuzzy rules are increased in the FWN, it results in more parameters and more computation, but can give better approximation accuracy than the other networks.

The training performance index and all network structures for all PV module types are summarized in Table 3. The optimal size of the FWN is determined for each solar cell technology by observing the performance index. Consequently, all cases were trained by using the FWN with 114 unknown free parameters which are constituted by taking as $M = 6$, $K = 4$, and $L = 1$ in the Eq. (1). At each training epoch, the performance index is calculated for both the training set and the test set. The training procedure is applied iteratively until a specified error goal is met. The algorithm converges very quickly and epoch number is 50 for all cases and the relationship between the training performance index of FWN and the number of the iteration is given in Fig. 8.

After the training process, the proposed method is validated with four different scenarios in order to show the learning capability of the networks for the new data sets. These operating conditions may represent the daily operation condition ofthe PV system. These operating conditions are obtained by using ramp, random number, repeating sequence and uniform random number signals. The ramp and repeating sequence signals represent the quick changes in irradiance and cell temperature, while the other two signals represent the slow changes in irradiance and cell temperature. The input signals

Table 3
Performance index of training process and network structures.

PV modules	RBF		ANFIS		TFFN		FWN			
	n_h	J	n_h	J	n_h	J	M	K	L	J
MST-43MV	12	0.018943	21	0.064521	4	0.037144	6	4	1	0.00092537
US-32	4	0.165788	21	0.015515	4	0.072516	6	4	1	0.00029961
ST-40	5	0.120026	21	0.053423	4	0.058335	6	4	1	0.00028179
FS-50	11	0.086174	21	0.15079	7	0.100284	6	4	1	0.00073969

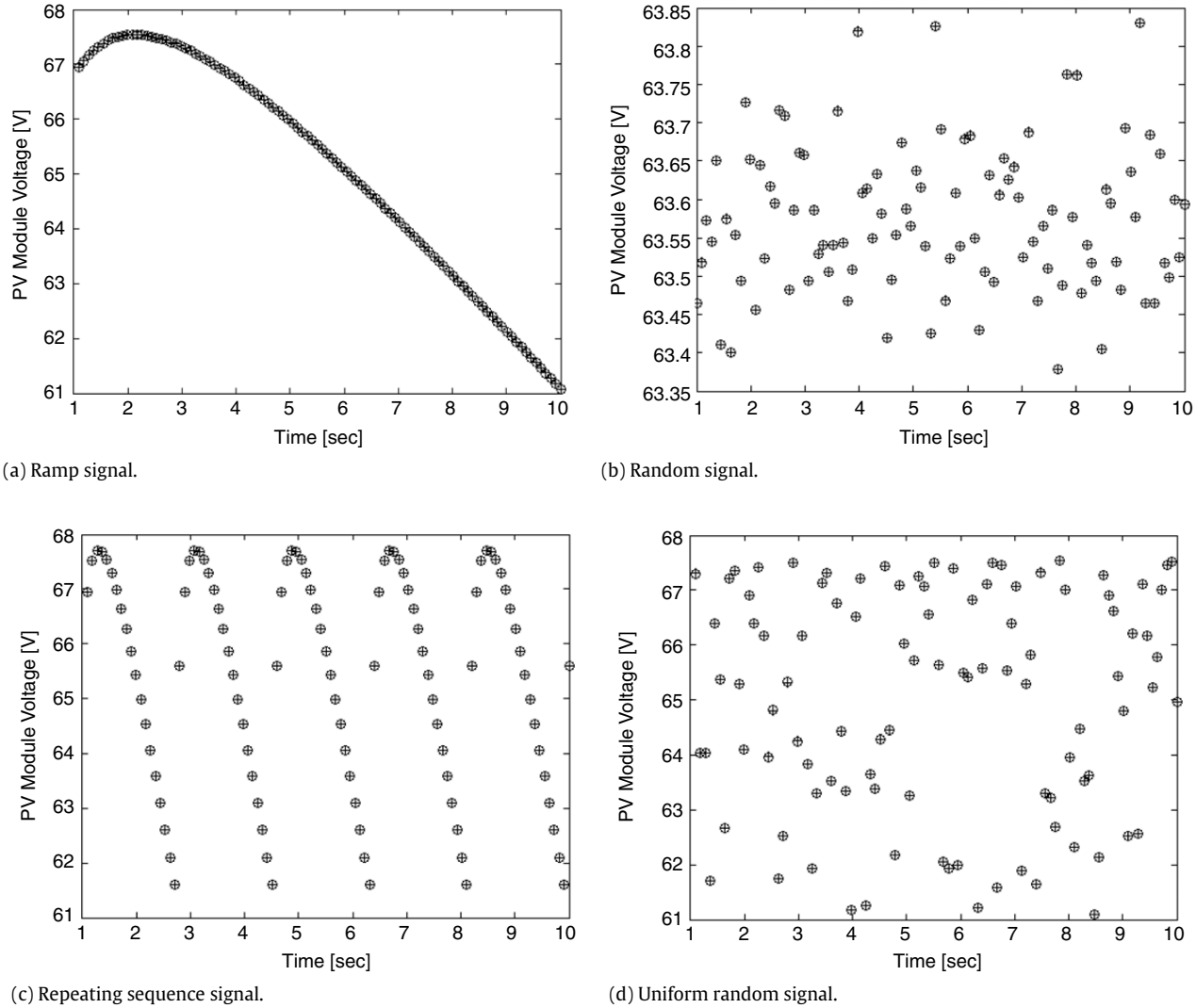

(a) Ramp signal.

(b) Random signal.

(c) Repeating sequence signal.

(d) Uniform random signal.

Fig. 9. Testing results of FWN network for FS-50 PV module ("○" ideal, "+" estimated values).

are defined as follows:

a. Ramp signal;
   $E = 90t + 100$ (W/m^2) and $T_c = 5.5t + 10$ (°C); for $0 < t < 10$ s.
b. Random number; where the mean of E and T_c are 800 W/m^2 and 50 °C, respectively, with variance = 1.0
c. Repeating sequence;
   $E = 450t + 100$ (W/m^2) and $T_c = 27.5t + 15$ (°C); for the periodic time $0 < t < 2$ s with 10 s of time simulation. where the periodic time (t) is 2 s with 10 s of time simulation
d. Uniform random number; $E_{\min} = 100$ W/m^2 and $E_{\max} = 1000$ W/m^2 and $T_{c\text{-min}} = 10$ °C and $T_{c\text{-max}} = 65$ °C.

One of the typical results of using the FWN for all types of input signals for FS-50 PV module is shown in Fig. 9. As shown in this figure, the FWN can identify the optimum voltage very close to the ideal one V_{MPP} for all types of input signal. This

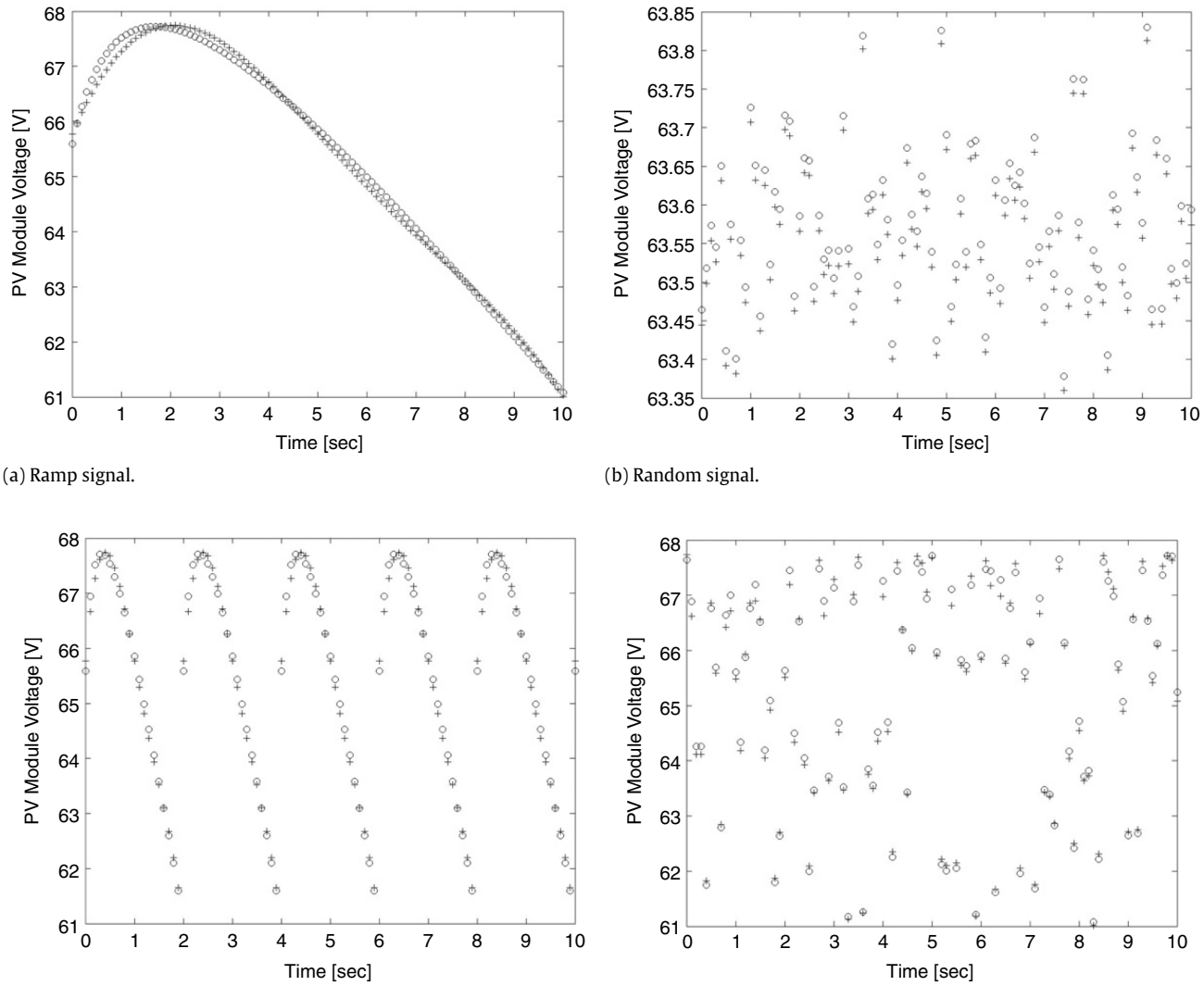

(a) Ramp signal.

(b) Random signal.

(c) Repeating sequence signal.

(d) Uniform random signal.

Fig. 10. Testing results of the RBF network for the FS-50 PV module ("○" ideal, "+" estimated values).

result indicates the accuracy of the FWN network in identifying the optimum point in the simple approach. This method is showing the same robustness for different PV module technologies and can adapt the new data set. For comparison, the FS-50 PV module is selected for the reason that this type of module is the most difficult task during the training process for RBF, ANFIS and TFFN networks in terms of high training error and instability of the training process.

As shown in Fig. 10, the RBF network seems to have spiraling identification around the optimum point under ramp signal input for FS-50 PV module. The same problem occurs in repeating sequence signal under low irradiance and cell temperature. This implies that RBF network is less suitable for a fast changing irradiance condition. On the other hand, a much worse approximation result is obtained using the ANFIS network. As shown in Fig. 11, the ANFIS structure almost fails to identify the optimum point for the ramp signal. Also, the high error validation occurs for a random number. This result is actually already predicted during the training process. It was explained from the performance index point of view during the training process that the ANFIS network causes an increase in the error and instability of the training process for the FS-50 PV module. For the TFFN network as shown in Fig. 12, this model has also some problems when dealing with the ramp signal, especially under high irradiance and cell temperature. Also it causes a high validation error when dealing with a random number. Again, this problem was identified as an unstable condition during the training process using the TFFN network for the FS-50 PV module.

The overall performance index of V_{MPP} estimation using the RBF, ANFIS, TFFN and FWN structures for all PV modules is presented in Table 4. The FWN network is able to map the optimum point for all types of non-c-Si PV modules. The other three network structures may only show good performance for individual types of PV module. The results confirm that the RBF method is likely suitable to map between the optimum voltage and the input signals for 2*ja*-Si cell technology. On the

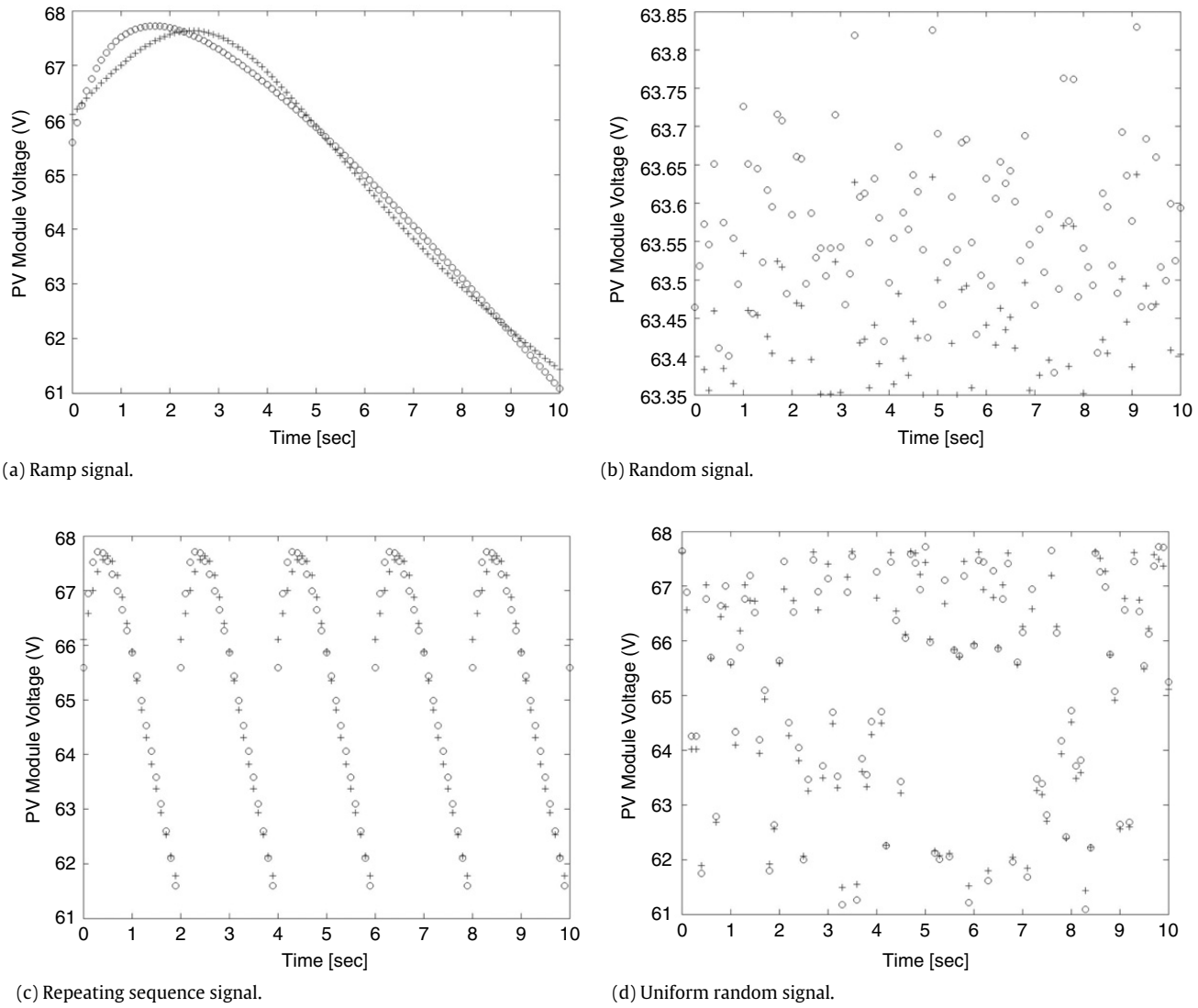

(a) Ramp signal.

(b) Random signal.

(c) Repeating sequence signal.

(d) Uniform random signal.

Fig. 11. Testing results of the ANFIS network for the FS-50 PV module ("○" ideal, "+" estimated values).

Table 4
Performance index for testing process.

PV modules	Ramp signal				Random signal			
	RBF	ANFIS	TFFN	FWN	RBF	ANFIS	TFFN	FWN
MST-43MV	0.03454	0.09636	0.06536	0.0015325	0.25768	0.98192	0.99178	0.0038753
US-32	0.14272	0.00713	0.05947	0.0001215	2.47386	0.03562	0.41765	0.0005786
ST-40	0.22127	0.14571	0.14312	0.0006126	1.91209	1.00343	1.02298	0.0069164
FS-50	0.06307	0.11509	0.08067	0.0006292	0.20480	2.00884	0.86844	0.0014228
	Repeating sequence signal				Uniform random signal			
MST-43MV	0.03534	0.11263	0.06955	0.0015938	0.03543	0.09170	0.06528	0.0015724
US-32	0.12771	0.00738	0.05875	0.0001909	0.14609	0.00778	0.05978	0.0001356
ST-40	0.23602	0.17081	0.15789	0.0012533	0.21687	0.13697	0.14579	0.0006412
FS-50	0.07109	0.13341	0.06372	0.0006447	0.06703	0.11191	0.07964	0.0006122

other hand, the ANFIS network is effectively used in the 3*j* a-Si technology. In other results, ANFIS and TFFN methods are giving similar responses in CIS technology; while RBF and TFFN methods are producing the same outcomes in thin film CdTe technology.

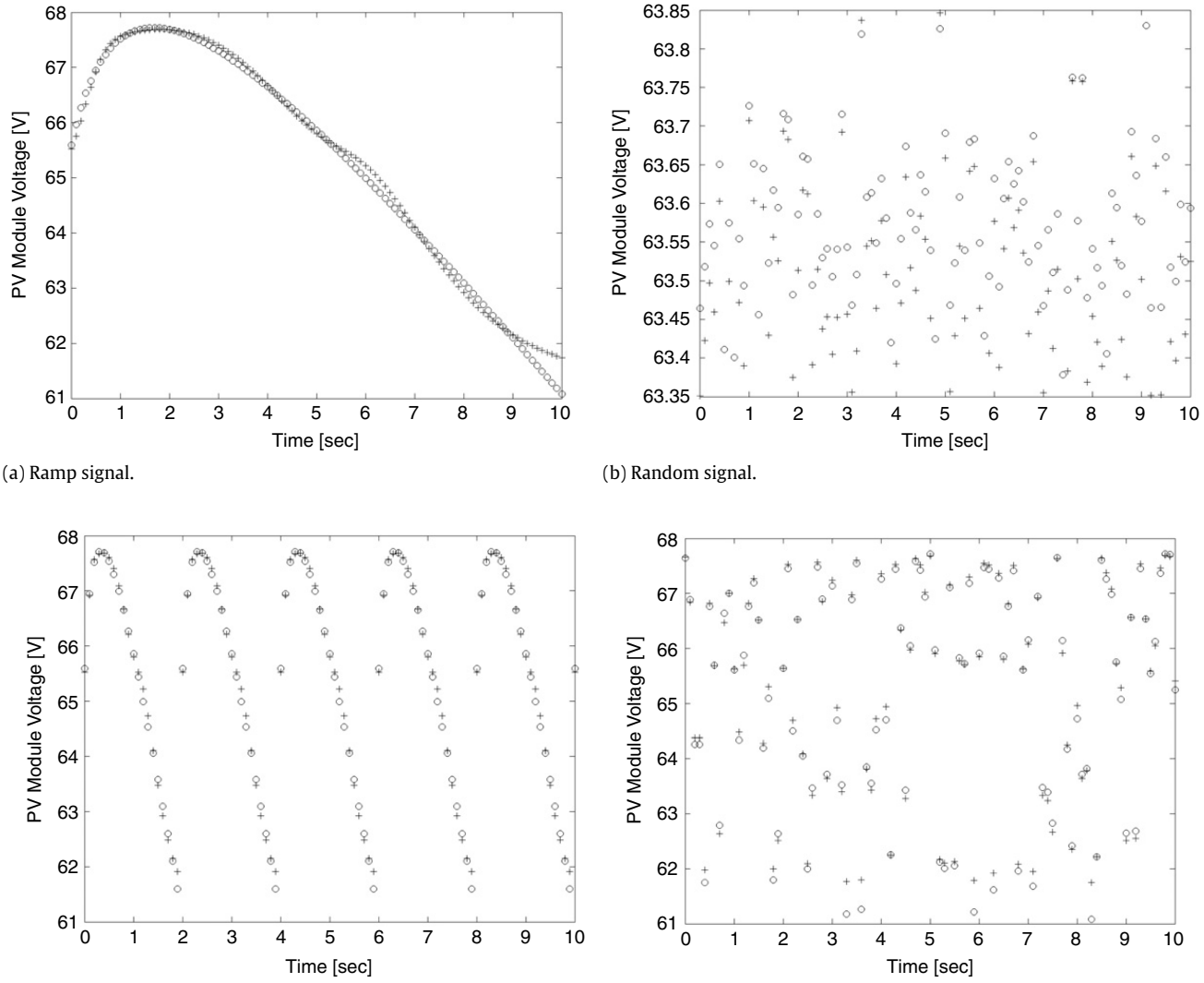

(a) Ramp signal.

(b) Random signal.

(c) Repeating sequence signal.

(d) Uniform random signal.

Fig. 12. Testing results of the TFFN network for the FS-50 PV module ("○" ideal, "+" estimated values).

5. Conclusion

This paper has investigated the eminence of the fuzzy wavelet network (FWN) dealing with the optimum operating point voltage estimation of non-crystalline Si PV modules. The results indicate that the combined fuzzy-wavelet approach allows a guarantee of very good tracking of the optimum operating point of different solar cell technologies under the different operating conditions. The proposed FWN is compared with the most commonly used ANN structure in PV system applications, such as RBF, ANFIS and TFFN. The trained configurations are verified using ramp, random, repeating sequence and uniform random signals of irradiance and cell temperature. The single FWN architecture can be enough to map the relationship between irradiance and temperature and optimum operating point voltage for all types of solar cells. The FWN can converge and adapt to new data sets with high accuracy. The performance of other ANN structures varies according to PV module types and operating conditions. For instance, RBF and ANFIS models are more suitable for 2*ja*-Si and 3*j* a-Si PV modules, respectively. On the other hand, ANFIS and TFFN are effectively used in CIS technology. For thin film CdTe technology, the RBF and TFFN methods are the best options.

Appendix. Supplementary data

Supplementary material related to this article can be found online at doi:10.1016/j.camwa.2011.10.073.

References

[1] A. Mellit, S.A. Kalogirou, Artificial intelligence techniques for photovoltaic applications: A review, Progress in Energy and Combustion Science 34 (2008) 574–632.

[2] A. Mellit, S.A. Kalogirou, L. Hontoria, S. Shaari, Artificial intelligence techniques for sizing photovoltaic systems: A review, Renewable and Sustainable Energy Reviews 13 (2009) 406–419.
[3] E. Karatepe, M. Alci, A new approach to fuzzy wavelet system modeling, International Journal of Approximate Reasoning 40 (2005) 302–322.
[4] Q. Zhang, A. Beveniste, Wavelet networks, IEEE Transactions on Neural Networks 3 (1992) 889–898.
[5] S. Yilmaz, Y. Oysal, Fuzzy wavelet neural network models for prediction and identification of dynamical systems, IEEE Transactions on Neural Networks 21 (2010) 1599–1609.
[6] M. Davanipoor, M. Zekri, F. Sheikholeslam, Fuzzy wavelet neural networks with hybrid algorithm in nonlinear system identification, in: Proceeding of the 2011 IEEE International Conference on Computer Science and Automation Engineering, 2011, pp. 153–156.
[7] A. Ebadat, N. Noroozi, A.A. Safavi, S.H. Mousavi, New fuzzy wavelet network for modeling and control: The modeling approach, Communications in Nonlinear Science and Numerical Simulation 16 (2011) 3385–3396.
[8] A. Al-Khazraji, N. Essounbouli, A. Hamzaoui, A robust adaptive fuzzy wavelet network based controller for a class of non-linear systems, International Journal of Modelling, Identification and Control 12 (2011) 290–303.
[9] N. Sadati, B. Marami, Fuzzy wavelet modeling using data clustering, in: Proceedings of the IEEE Symposium on Computational Intelligence and Data Mining, 2007, pp. 114–119.
[10] M. Shangchang, T. Zanma, M. Ishida, Identification of human skill and its application to an automatic driving system—An approach from hybrid dynamical system, IECON Proceedings on Industrial Electronics Conference (2006) 400–405.
[11] F. Giraud, Z.M. Salameh, Analysis of the effects of a passing cloud on a grid-interactive photovoltaic system with battery storage using neural networks, IEEE Transactions on Energy Conversion 14 (1999) 1572–1577.
[12] X. Sun, W. Wu, X. Li, Q. Zhao, A research on photovoltaic energy controlling system with maximum power point tracking, IEEE Proceeding of the Power Conversion Conference (2002) 822–826.
[13] A. Mellit, M. Benghanem, S.A. Kalogirou, An adaptive wavelet-network model for forecasting daily total solar-radiation, Applied Energy 83 (2006) 705–722.
[14] B. Cao, L. Chang, H. Li, Implementation of the RBF neural network on a SOPC for maximum power point tracking, in: Proceeding of the Canadian Conference on Electrical and Computer Engineering, 2008, pp. 981–985.
[15] A. Yona, T. Senjyu, A.Y. Saber, T. Funabashi, H. Sekine, K. Chul-Hwan, Application of neural network to 24-h-ahead generating power forecasting for PV system, in: Proceeding of the Power and Energy Society General Meeting–Conversion and Delivery of Electrical Energy in the 21st Century, 2008, pp. 1–6.
[16] S. Zhou, L. Kang, G. Guo, Y. Zhang, J. Cao, B. Cao, The application of combinatorial optimization by genetic algorithm and neural network, in: Proceeding of the 3rd IEEE Conference on Industrial Electronics and Applications, 2008, pp. 227–231.
[17] S. Zhou, L. Kang, G. Guo, Y. Zhang, B. Cao, The combinatorial optimization by genetic algorithm and neural network for energy storage system in solar energy electric vehicle, in: Proceeding of the 7th World Congress on Intelligent Control and Automation, 2008, pp. 2838–2842.
[18] A. Varnham, A.M. Al-Ibrahim, G.S. Virk, D. Azzi, Soft-computing model-based controllers for increased photovoltaic plant efficiencies, IEEE Transactions on Energy Conversion 22 (2007) 873–880.
[19] A. Mellit, S.A. Kalogirou, Neuro-fuzzy based modeling for photovoltaic power supply system, in: Proceeding of the First International Power and Energy Conference, 2006, pp. 88–93.
[20] J.S. Choi, D.Y. Kim, K.T. Park, J.H. Choi, D.H. Chung, Tracking system and MPPT control for efficiency improvement of photovoltaic, in: Proceeding of the International Conference on Control, Automation and Systems, 2008, pp. 1341–1344.
[21] Y. Narri, V. Mummadi, Adaptive controller for PV supplied buck-boost converter, in: Proceeding of the IEEE International Conference on Power Electronics and Drive Systems, 1999, pp. 789–793.
[22] K. Jae-Sub, J. Byung-Jin, P. Ki-Tae, C. Chung-Hoon, C. Dong-Hwa, Maximum power point tracking control of PV system for DC motors drive with neural network, in: Proceeding of the International Conference on Smart Manufacturing Application, 2008, pp. 514–519.
[23] A. de Medeiros Torres, F.L.M. Antunes, F.S. dos Reis, An artificial neural network-based real time maximum power tracking controller for connecting a PV system to the grid, in: Proceeding of the 24th IEEE Annual Conference on Industrial Electronics Society, 1998, pp. 554–558.
[24] J.A. Momoh, Y. Wang, F. Eddy-Posey, Optimal power dispatch of photovoltaic system with random load, in: Proceeding of the IEEE Power Engineering Society General Meeting, 2004, pp. 1939–1945.
[25] S. Chakraborty, M.G. Simoes, PV-microgrid operational cost minimization by neural forecasting and heuristic optimization, in: Proceeding of the IEEE Industry Applications Society Annual Meeting, 2008, pp. 1–8.
[26] S.I. Sulaiman, T.K. Abdul Rahman, I. Musirin, Optimizing one-hidden layer neural network design using evolutionary programming, in: Proceeding of the 5th International Colloquium on Signal Processing & Its Applications, 2009, pp. 288–293.
[27] G. Tina, G. Capizzi, Improved lead-acid battery modeling for photovoltaic application by recurrent neural networks, in: Proceeding of the International Symposium on Power Electronics, Electrical Drives, Automation and Motion, 2008, pp. 1170–1174.
[28] M.G. Villalva, J.R. Gazoli, E.R. Filho, Comprehensive approach to modeling and simulation of photovoltaic arrays, IEEE Transactions on Power Electronics 24 (2009) 1198–1208.
[29] H.G. Beyer, R. Gonschalg, T.R. Betts, D.G. Infield, Modeling the realistic short circuit current and MPP power of a-Si single and multijunction devices, in: Proceeding of the 3rd World Conference on Photovoltaic Energy Conversion, 2003, pp. 2435–2438.
[30] Syafaruddin, E. Karatepe, T. Hiyama, Polar coordinated fuzzy controller based real-time maximum power point control of photovoltaic system, Renewable Energy 34 (2009) 2597–2606.
[31] Syafaruddin, E. Karatepe, T. Hiyama, Artificial neural network polar coordinated fuzzy controller based maximum power point tracking control under partially shaded conditions, IET Renewable Power Generation 3 (2009) 239–253.
[32] M. Thomson, D.G. Infield, Impact of widespread photovoltaics generation on distribution systems, IET Renewable Power Generation 1 (2007) 33–40.
[33] D.L. King, Photovoltaic module and array performance characterization methods for all system operating conditions, in: Proceedings of NREL/SNL Photovoltaics Program Review Meeting, 1997, pp. 1–22.
[34] D.L. King, Sandia's PV module electrical performance model, Sandia National Laboratories, September 2000.
[35] C.B. Sidney, R.A. Gopineth, H. Guo, Introduction to Wavelets and Wavelet Transforms, Prentice Hall, 1998.
[36] Junghui Chen, Duane D. Bruns, WaveARX neural network development for system identification using a systematic design systematic design synthesis, Industrial and Engineering Chemistry Research 34 (1995) 4420–4435.
[37] S. Yao, C.J. Wei, Z.Y. He, Evolving wavelet neural networks for function approximation, Electronics Letters 32 (1996) 360–361.
[38] X. Song, J. Chen, F. Qi, A new way of setting initial parameter value for fast convergence wavelet neural network used for signal or function approximation, Journal of Infrared and Milimeter Waves 16 (1997) 33–38.
[39] A.A. Safavi, J.A. Romagnoli, Application of wavelet based neural networks to modeling and optimization of an experimental distillation column, Engineering Application of Artificial Intelligence 10 (1997) 301–313.
[40] D.W.C. Ho, P.A. Zhang, J. Xu, Fuzzy wavelet networks for function learning, IEEE Transactions on Fuzzy Systems 9 (2001) 200–211.
[41] S. Srivastava, M. Singh, M. Hanmandlu, A.N. Jha, New fuzzy wavelet neural networks for system identification and control, Applied Soft Computing 6 (2005) 1–17.
[42] J. Wang, J. Xiao, H. Peng, X. Gao, Constructing fuzzy wavelet network modeling, International Journal of Information Technology 11 (2005) 68–74.
[43] N. Sadati, B. Marami, Fuzzy wavelet modeling using data clustering, in: Proceedings of the IEEE Symposium on Computational Intelligence and Data Mining, 2007, pp. 114–119.
[44] M. Singh, S. Srivastava, M. Hanmandlu, J.R.P. Gutpa, Type-2 fuzzy wavelet networks (T2FWN) for system identification using fuzzy differential and Lyapunovstability algorithm, Applied Soft Computing 9 (2009) 977–989.

[45] S. Tzeng, Design of fuzzy wavelet neural networks using GA approach for function approximation and system identification, Fuzzy Sets and System 161 (2010) 2585–2596.
[46] A. Ebadat, N. Noroozi, A.A. Safavi, S.H. Mousavi, New fuzzy wavelet network for modeling and control: The modeling approach, Communications in Nonlinear Science and Numerical Simulation 16 (2011) 3385–3396.
[47] Z. Zainuddin, P. Ong, Modified wavelet neural network in function approximation and its application in prediction of time-series pollution data, Applied Soft Computing (2011). doi:10.1016/j.asoc.2011.06.013.
[48] Q.J. Guo, H.B. Yu, A.D. Xu, A hybrid PSO-GD based intelligent method for machine diagnosis, Digital Signal Processing 16 (2006) 402–418.
[49] A. Mellit, M. Menghanem, M. Bendekhis, Artificial neural network model for prediction solar radiation data: application for sizing stand-alone photovoltaic power system, in: Proceeding of the IEEE Power Engineering Society General Meeting, 2005, pp. 40–44.
[50] K. Hyun-Soo, B.G. Morris, H. Seung-Soo, G.S. May, A comparison of genetic and particle swarm optimization for contact formation in high-performance silicon solar cells, in: Proceeding of the IEEE International Joint Conference on Neural Networks, 2008, pp. 1531–1535.
[51] Syafaruddin, E. Karatepe, T. Hiyama, ANN based real-time estimation of power generation of different PV module types, IEEJ Transaction on Power and Energy 129 (2009) 783–790.